971469

Low Speed Canard-Tip-Vortex Airfoil Interaction

R. Mahalingam, R. B. Funk, and N. M. Komerath
Georgia Institute of Technology

ABSTRACT

This paper describes a series of ongoing experiments to capture the details of perpendicular vortex-airfoil interaction. Three test cases explored are: 1) a 21% thick symmetric airfoil at -1.1° angle of attack, 2)a thin flat plate of 2.5% thickness with rounded leading edge, sharp trailing edge and zero angle of attack and 3) A 12% thick symmetric airfoil at zero angle of attack. The tip vortex was generated by a NACA0016 wing at 5° AOA. The strength of the vortex was computed from the velocity profile measured upstream for the first two cases. Pressure measurements on the 21% airfoil were used to quantify the effect of the vortex as a function of its stand-off distance from the airfoil. Vortex trajectories over the airfoils were obtained from laser sheet videography. The vortex motion conforms to potential flow expectations except in regions of pressure gradient and during head-on interaction. When the generating wing is moved continuously across the airfoil there is a time lag between wing and vortex motion. The vortex switching from the top to the bottom surface is initiated by the splitting of the primary vortex into two and occurs in a short period of time. This is a source of unsteady effects on the interacting airfoil and a vortex jump parameter is defined for the switching process. Issues regarding symmetry in the motion above and below the airfoils are discussed.

INTRODUCTION

The wing-airfoil interaction relates to various problems. Lombardi[1] reports the problem where the vortex from a canard interacts with the main wing(Fig.1a). This is primarily a quasi-steady interaction, but can also involve sudden loads and moments during maneuvers such as landing and pitch-up due to vortex switching across the surface of the interacting wing. Vortex switching can reduce control surface effectiveness and even produce control reversal over short periods of time. Computational simulation of the flow with small stand-off distances between the vortex and the airfoil is complicated and expensive because of the viscous effects involving both the vortex and boundary layer on the interacting airfoil. A similar problem is the interaction of flap vortices with horizontal tails and with the ground during landing and take-off. Yu [2] summarizes the large body of research conducted on the problem of blade-vortex interaction (BVI, Fig. 1b) encountered by rotorcraft during descent. This occurs on a short time scale and causes sharp pressure pulses which propagate. This is a source of noise and therefore a limiting factor in the community acceptance of helicopters. Tung and Yu [3] review the aerodynamic aspects of BVI. Other applications are in the interaction of vortices from different wings of a micro air vehicle, or between the rotor tip vortex of a rotorcraft with downstream stabilators or other surfaces. The understanding of the fluid-dynamics of vortex-surface interactions is obviously very important for various ground-based transportation systems, in areas like noise reduction and drag reduction on following vehicles. Nouzawa et al. [4] describe work done on unsteady-wake analysis on the bluff flow behind a model for drag reduction. Haruna et al.[5] have studied the aerodynamic noise from 3-D wings.

The previous work in this area is quite extensive, but done with various types of diagnostics and motivated by various applications. Patel and Hancock[6] conducted visualization and pressure measurements on the interaction of a tip vortex with a wing. Low-speed studies by Seath and Wilson [7] documented a significant change in the pressure distribution of the interacting airfoil and noticed a spanwise drift. Kalkhoran etal [8] studied the interaction details at transonic Mach Nos. and concluded that there is an unsteadiness associated with the location of the vortex core. The closeness of the vortex to the interacting airfoil was an important parameter while Reynolds Number was not. They noticed the formation of two vortical regions during close interactions, which they associated with the formation of a secondary vortex or vortex-splitting. Ref[9] describes the work done recently on this interaction at the authors' organization.

This includes vortex trajectories and flow-visualization on the flat plate airfoil.

Cutler and Bradshaw [10] have studied the interaction between a longitudinal vortex pair and a turbulent boundary layer on a plate. Wittmer and Devenport ([11], [12]) did a series of experiments on a similar configuration. Ref. [13], by the same authors, describes turbulence measurements on a similar configuration. They concluded that negative vorticity is shed in the airfoil wake due to the vortex load and this imparts an unstable circulation distribution to the vortex. They also found that the blade wake is distorted considerably.

SCOPE AND OBJECTIVES

Our original motivation for studying this problem was as a test case of a slow vortex-body interaction, where the characteristic dimension of the obstacle was of the same order as the vortex core size. This fell somewhere between the rotor/airframe collision (obstacle size >> vortex core), and the BVI problem (obstacle size < core size). The perpendicular interaction being studied here is quasi-steady, but three-dimensional. The axial velocity in the vortex core is small relative to the swirl velocity and the filament has little curvature. The flow-visualization was conducted at a Reynolds number of 279,000 based on the chord of the vortex generator. Some of the pressure measurements shown here were at Reynolds number of 1.4 million.

A simple test case is explored for the quasi-steady interaction between a wing tip vortex and a downstream airfoil. Two airfoils almost spanning the wind tunnel test section were tested; one a 21% thick airfoil, and the other a thin flat plate with a rounded leading edge and a sharp trailing edge. A third test case, being currently done in a 42" x 42" tunnel as an undergraduate class project with a different vortex generator and a different full-span airfoil [14], is being used to provide qualitative answers to some questions arising from the previous experiments.

In Ref [9] we described the flow visualization results on the first two airfoils, which are repeated here for continuity. Surface pressure measurements are reported here, and related to the flow visualization. Unsteady effects in the interaction are identified.

Types of experiments

1. The generating wing, henceforth called the Vortex Generator(VG) was held at a fixed location and flow-visualization and surface-pressure measurements were performed on a thick airfoil.
2. The VG was moved vertically at a constant, slow rate to provide a quasi-steady interaction with the flat plate and the interaction was visualized in specified spanwise vertical planes using a laser sheet illuminating smoke.

The interaction is divided into three phases. When the vortex is more than one core diameter away from the surface of the airfoil the interaction behaves according to potential flow expectations and hence this phase is called the potential phase(PP). When the vortex is less than one core diameter from the airfoil the interaction is termed as a close-interaction phase(CIP). When the vortex is nominally in the plane of the airfoil the interaction is termed as the head-on interaction phase (HIP).

The main issues of interest were:

1. The effect of the vertical stand-off distance between the VG and the airfoil.
2. Vortex-switching unsteadiness and reduced frequency for the switching.
3. Effect of pressure gradient on the vortex motion.
4. For the CIP, effect of the airfoil thickness on the vortex behaviour.
5. Symmetry issues.

EXPERIMENTAL METHOD

The experiments were carried out in the J.J.Harper wind-tunnel and in the Low-Turbulence Wind Tunnel(LTWT) at Georgia Tech. The Harper tunnel is a low speed, closed-circuit tunnel with freestream turbulence levels of less than 0.5%. The test section has a 2.13m by 2.74m cross-section. The LTWT is a blow-down tunnel with a square test-section of 1.07m side. The vortex generator (VG) was a 16%, symmetric airfoil-section, semi-span wing of aspect ratio 4.26 and 0.14m chord, placed 6.5 VG-chord lengths upstream of the airfoil. The VG was moved vertically through $-0.146 < VGz/c < 0.146$. The experimental setup and coordinate system are shown in Fig.2a. The flat-plate airfoil had span 2.44m, chord 0.52m, and thickness 1.3cm. The LE of the flat-plate was rounded, so that there was curvature upto $x/c = 0.037$. A sharp trailing edge was provided. The sharp trailing edge resulted in a slope on the surface for $0.9 < x/c < 1.0$. Effects that gradients might introduce in the vortex trajectories were expected to be seen around the leading and trailing edges. The flat plate was at zero angle of attack for all the runs The VG angle of attack was held fixed at 5° for all the results presented here. The free-stream velocity was 3.048 m/s (10 ft/s) for the flow-visualization and 15.24 m/s (50 ft/s) for the pressure measurements. The thick airfoil was a NACA0021 airfoil section with a span of 2.23 m and a chord 0.4 m. The AOA of the thick airfoil was 1.1°. The third airfoil is a full-span 12% thick airfoil at zero angle of attack. Even though both the flat-plate and the thick airfoil were not full span and therefore, not strictly airfoils, the region of interest on them was limited to the center part. With the aspect ratio of 5.5, the end effects in the middle are negligible. Hence, reference is made throughout the paper to airfoils.

Velocity Measurements

The velocity profile of the vortex was measured using a laser velocimeter. A TSI fiber-optic probe transmitted the dual-beam with the unshifted beam at 514 nm (green). The scattered light was collected in back-scatter by the same probe and conveyed to a photomultiplier. The photomultiplier signal was downmixed and was processed by a TSI 1990 counter. A TSI 1998 interface was used to transfer the data to a Gateway 2000 486/66 computer. The flow was seeded using mineral oil from an atomizer placed downstream of the test-section. An approximate location for the vortex core was established from flow visualization in vertical, spanwise planes at 7.6 (x/c=-0.293) and 6.5 (x/c=-0.585) VG-chord lengths behind the trailing edge of the VG. The vertical velocity component was measured along a spanwise line passing through the center of the core. The velocity profile of the vortex was used to

estimate the circulation in the vortex from the velocities at the end points of diameter along which the vertical velocity components were measured. Knowing the center of the vortex, the circulation was obtained.

Pressure Measurements

Since the flow was expected to be primarily steady the upper surface pressure was used as a criterion to quantify the effect of the vertical vortex stand-off distance from the airfoil. This was achieved by static pressure ports on the surface and Barocel pressure transducers mounted outside the test-section. The data acquisition program sampled both the tunnel dynamic and model surface pressure transducers 50,000 times at 2000 Hz.

Flow Imaging

The flow was illuminated using a light sheet from a 30watt Copper Vapor laser operating at 6000, 25-nanosecond pulses per second. The video signal was recorded from an intensified video camera placed downstream of the test section. The camera was initially aligned by focussing on a grid board with scale markings, placed in the plane of the laser sheet. The grid-board also provided the scaling factor for transfering vortex locations from screen-coordinates to physical coordinates. Fig. 2b shows a schematic of the data acquisition procedure for imaging.

Instantaneous flow images of spanwise-vertical planes were digitized from video throughout the interaction period at several locations along the chord. Selected stills from the sequence are presented here to describe different phases of the collision process along the top and bottom surface of the interacting surface. Entire three-dimensional vortex trajectories were derived from these frames. This was done by locating the vortex core position on the screen coordinates and transferring that location to real space coordinates.

RESULTS

Vortex characteristics

Fig. 3 shows the vertical component of the velocity across the vortex. The tip vortices have almost completely rolled up by x/c = -0.585 and the value of circulation obtained is 0.094 m^2/s. Further roll-up has occured by x/c = -0.293 and the circulation has increased to 0.099 m^2/s. The vortex core diameter has not changed appreciably from x/c = -0.585 to x/c = -0.293. This established that by the time the vortex interacted with the airfoil it was a well-developed, rectilinear vortex of constant core diameter. The vortex core diameter at the LE of the airfoil is about 2.0 cm, (14% of the chord length of the VG), which is of the order of the flat-plate thickness. Fig. 3b. shows the theoretical circulation distribution calculated from finite-wing lifting-line theory of Prandtl. The peak circulation is about 0.094 m^2/s matches the measured vortex circulation very well.

Vortex motion on the 21%thick airfoil

These results have been presented in Ref. 9., and have been repeated here for continuity. Fig. 4 shows the vortex trajectories on the top surface of the thick wing as obtained from both pressures and flow-visualization. The thickness of the wing prevented simultaneous visualization on the bottom surface. The results show lateral movement of the vortex according to potential theory of images. Such a simple theory is still valid as the vortex is not yet close to the surface and its motion is quasi-steady. Motion of the vortex in only two-planes is shown for the sake of clarity. Note that the two planes shown in the figure are ahead of the maximum thickness point and are in a region of favourable pressure gradient. An interesting, and perhaps counterintuitive, feature is that the lateral movement is highest at the LE. Since the vortex filament is continuous, one might expect that as we go downstream of the LE the vortex tends to move further to the left. This gave us an indication that the pressure gradient might have an effect that causes a vortex motion opposite to that predicted by image-vortex theory.

Vortex motion on the flat plate

Vortex-trajectories derived from flow-visualization are presented in Ref. 9. and are available in electronic form for computational comparisions. Fig. 5. summarizes the three phases of the interaction. When the vortex is about one-half core diameter above the top surface, it is approximately at the end of the PP.

Growth in core size

There is a significant, continuous increase in the core size from the LE to the TE. There is a sudden increase in the core size from x/c=1.0 to x/c = 1.39 accompanied by the vortex core diffusing out. Fig. 6 describes growth in core size relative to the size at the LE, from LE to the TE, for a Vgz/c = 0.0.

Unsteady vortex-splitting and switching phenomenon

For the HIP the vortex splits into two. At x/c = 0.171 the vortex appears cut in two. Further downstream the individual split-up parts roll up to form two distinct circulatory regions above and below the airfoil. These regions diffuse out and breakdown by x/c = 0.9. The sense of circulation of the split-up vortices is same as the parent vortex. The secondary vortices diffuse much before the parent vortex does and this would indicate lower vorticity and a closer interaction for them.

It is interesting to note that there was no appreciable unsteadiness in the vortex core position during either the PP or the CIP. During the HIP, however, the vortex appeared to flip between the upper and lower surface.

Fig. 7 shows the motion of the vortex in time with the motion of the VG. As the VG goes lower the vortex tends to stay above the airfoil, therefore increasing curvature of the vortex considerably before switching over to the bottom. Also, note that the jump across the airfoil is higher for successive planes downstream. This suggests a whip-like action of the vortex when it jumps across. This is actually seen in the video of the interaction.

Effect of Pressure gradient

It was noted on the thick airfoil that pressure gradient seemed to affect the vortex motion. Since our primary interest was to capture the vortex-switching mechanism we decided to use a thin flat-plate airfoil for visualizing both sides simultaneously. We later noticed that even on the flat-plate, the vortex motion was affected at the LE and the TE. This is

seen in Fig. 8. Note the opposite motions of the vortex at the LE and TE. At the LE in regions of favorable pressure the vortex motion is opposite to what is predicted by potential flow, while at the TE it is accelerated along the direction predicted by image vortex theory. This is only a preliminary finding and needs to be confirmed with further experimental studies and analytical methods.

Effect on vortex at the LE for the HIP

The size of the core in comparision has an effect on the vortex behavior during the HIP. For the flat-plate the vortex was cut in two regions, one staying above and the other below. For the thick airfoil, however the vortex appeared to stretch and breakdown at the LE.

Pressure measurement on the thick airfoil

Fig. 9 shows the effect of vortex closeness to the airfoil. Both the standoff distances (Vgz/c=0.0 and -0.0136) shown are such that the vortex is still above the upper surface of the airfoil. The pressure traces show a suction in the region under the vortex, which increases in magnitude as the vortex moves closer. Also note the difference in the pressure signature caused at the different streamwise locations. The most upstream traces show a stagnation region to the left of the primary suction. This might be an indication of the beginning of boundary layer separation. Fig. 10 shows the footprint of the vortex as seen from the pressure distributions.

Vortex jump parameter for the unsteady switching

Once the switching phenomenon was noted to be unsteady, the next issue was if we could define a parameter to quantify the unsteadiness. This is the vortex jump parameter which is defined as the ratio of the downward velocity of the vortex during the switching to the velocity of the VG. This parameter is plotted as a function of the streamwise position on the airfoil in Fig.11. This clearly indicates what we call as the "whip-like" action. This would lead to a time-varying pitching moment variation on the airfoil and even induce twisting loads.

Symmetry Issues

We are using the ongoing experiments to confirm some of the issues raised earlier. It was noted in Ref. 9 that the vortex trajectories above and below the airfoil are not symmetric. We had conjectured previously that the asymmetry might have been caused by the fact that the airfoil was closer to the bottom of the test-section. The current experiments are performed to ensure complete symmetry in the configuration, but even these show an asymmetry in the trajectories. When the angle of attack of the VG is made negative the asymmetry is repeated but as a mirror image of the positive angle of attack case. It appears that the asymmetry might be a result of the wing inboard-wake curvature.

Work is in progress to understand the various unresolved issues in the intercation. Primary amongst these are the effect of an unsteady maneuver on the vortex switching time scales, unsteady forces imparted over the vortex-switching region, identification of a boundary layer separation line under the vortex. Tuft visualization and pressure measurements will be used to isolate these phenomenon. Also attempts will be made to correlate the experimentally observed phenomenon with computations of the interaction.

CONCLUSIONS

Flow visualization is related to pressure measurements of a perpendicular, vortex-airfoil interaction. Previously we had concluded that

1. Effects of pressure gradient were noticed on the thick airfoil at the leading and trailing edges of the thin airfoil. In particular a favourable pressure gradient moves the vortex in a direction opposite to that by image vortex theory, and an adverse pressure gradient moves it in the same direction.
2. For a head-on collision the vortex is cut by the airfoil and there is an appearance of two vortices above and below the airfoil.
3. The vortex motion is steady but delayed with respect to the VG till it comes to the HIP. It continuously slows down, and then jumps across abruptly.

The new results show that

4. The vortex circulation obtained from LDV measurements matched well with the potential circulation distribution calculated on the VG.
5. There is an increase in core size from the LE to the TE, in the presence of an interacting airfoil.
6. The footprint of the vortex in the pressure the measurements shows the span-wise motion of vortex as it moves over the airfoil surface. Influence of the vortex increases as the stand-off distance decreases as seen from the suction magnitude.
7. A vortex-jump parameter has been defined for the vortex switching. It quantifies the whipping effect.
8. There is asymmetry in the trajectory even for a perfectly symmetric configuration. This might be a result of the wing inboard-wake curvature. The asymmetry is mirror imaged on setting the VG at a negative angle of attack.

ACKNOWLEDGMENTS

This work was performed under a subcontract from Ohio State University Foundation on ARO contract DAAH04-93-G-0048. Dr.T.L.Doligalski is the Technical Monitor. We are grateful to Dr. Terry Conlisk at Ohio St. U. for his advice and suggestions. We also thank Kevin Peterson and John Lynn for their help in the experiments.

REFERENCES

1. Lombardi, G., "Canard Tip Vortex Splitting in a Canard-Wing Configuration: Experimental Observations". Journal of Aircraft, Vol. 32, No. 4, July-August 1995, p. 875 - 877.
2. Yu, Y. H., "Rotor Blade-Vortex Interaction Noise: Generating Mechanisms and Control Concepts". Proceedings of the AHS 2nd International Aeromechanics Specialists' Conference, Bridgeport, CT, Vol. 1, October 1995, pp. 3-1 - 3-12.
3.Tung. C. and Yu, Y. H., Low, S. L., " Aerodynamic Aspects of BVI " AIAA 27th Fluid Dynamics Conference, AIAA paper 96-2010, New Orleans, LA.

4. Nouzawa, T., Hiasa, K., Nakamura, T., Kawamoto, A., and Sato, H., " Unsteady Wake Analysis of the Aerodynamic Drag of a Notch Back Model with Critical Afterbody Geometry", No. 920202, Vehicle Aerodynamics : Wake Flows, Computational Fluid Dynamics, and Aerodynamic Testing, SP-908, SAE Global Mobility Database.
5. Haruna, S., Hashiguchi, M., Kamimoto, I., and Kuwahara, K., " Numerical Study of Aerodynamic Noise radiated from a Three-Dimensional Wing" ,No.920341, Vehicle Aerodynamics : Wake Flows, Computational Fluid Dynamics, and Aerodynamic Testing, SP-908, SAE Global Mobility Database.
6. Patel, M.H., Hancock, G.J., Apr 1974, Some Experimental Results of the Effect of a Streamwise Vortex on a Two-Dimensional Wing, Aeronautical Journal, pp 151-155.
7. Seath, D.D., Wilson, D.R., Jan 1986, Vortex-Airfoil Interaction Tests, AIAA 24th Aerospace Sciences Meeting, AIAA Paper 86-0354, Reno, NV, Jan. '86.
8. Kalkhoran, I.M., Wilson, D.R., and Seath, D.S., "Experimental Investigation of the Perpendicular Rotor Blade-Vortex Interaction at Transonic Speeds". AIAA Journal. Vol. 30, No. 3, March 1992, pg 747-755.
9. Mahalingam, R., Funk. R.B., and Komerath, N.M., "Flow Visualization of Low Speed Perpendicular Vortex-Airfoil Interaction", AIAA 14th Applied Aerodynamics Conference, AIAA paper 96-2387, New Orleans, LA.
10. Cutler, A.D., and Bradshaw, P., " Strong Vortex/Boundary Layer Interactions", Experiments in Fluids, Vol. 14, , 1993, pg. 321-332.
11. Wittmer, K. S., and Devenport, W. J., " Interaction of a Streamwise Vortex with a Full-span Blade", AIAA paper 95-2214, June 1994.
12. Wittmer, K. S., and Devenport, W. J.," Perpendicular Blade Vortex Interaction", AIAA Journal, Vol 33, No. 9,Sept 1995, pg. 1667-1674.
13. Wittmer, K. S., and Devenport, W. J.,"Turbulence Structure resulting from a Perpendicular Airfoil-Vortex Interaction", AIAA paper 96-2014, 27th AIAA Fluid Dynamics Conference, June 1994 .
14. Wong, O., Gialloreto, V. B. , Hendricks, T., "Wing-wing interaction experiment test manual". Final report in AE4010 Advanced Flow Diagnostics, School of Aerospace Engineering, Georgia Institute of Technology, Atlanta, GA, Winter 1997.

DEFINITIONS, ACRONYMS, ABBREVIATIONS

c	chord of the flat-plate airfoil
Cp	Pressure coefficient
CIP	Close Interaction Phase
HIP	Head-on Interaction Phase
LE	leading edge of airfoil
M	Mach number
PP	Potential Phase
TE	trailing edge of airfoil
VG	vortex generator
VGz/c	vortex generator height relative to the coordinate system used
Vinf	freestream velocity
x, y, z	cartesian coordinates
x/c	non-dimensional distance along the chord of the airfoil
y/c	non-dimensional distance along the span of the airfoil
z/c	non-dimensional distance perpendicular to the surface of the airfoil
Γ	circulation

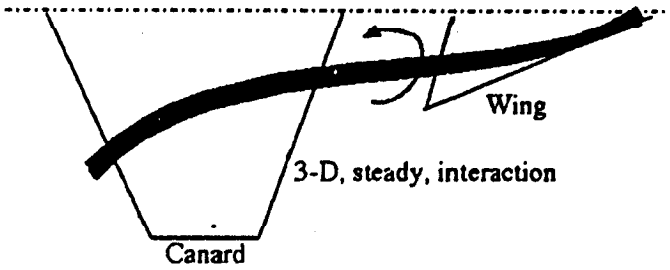

Fig. 1(a). Schematic of Canard-Wing interaction

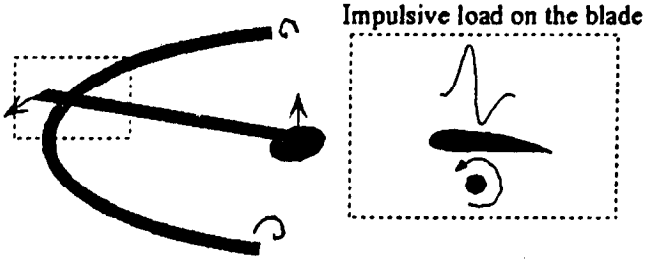

Fig. 1(b). Schematic of helicopter BVI

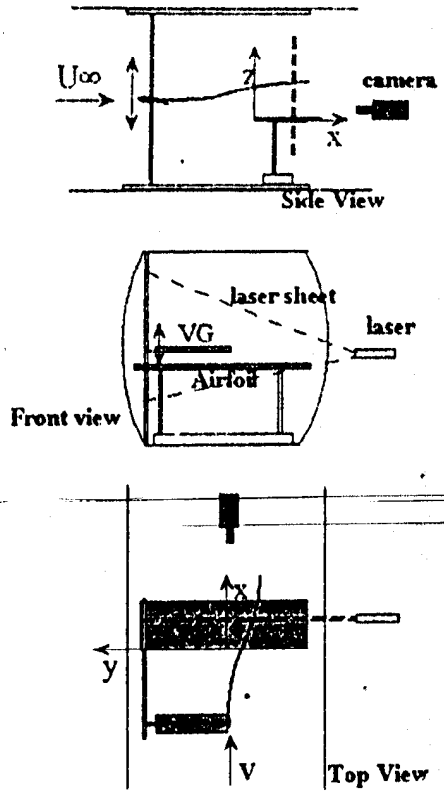

2(a). Experimental setup for the vortex airfoil intera
VG : Vortex Generator

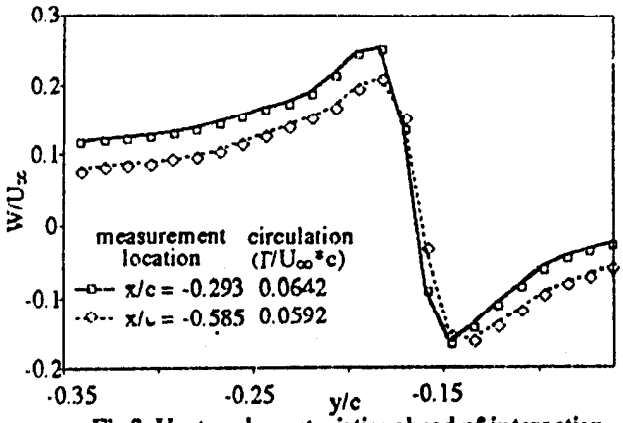

Fig.3. Vortex characteristics ahead of interaction

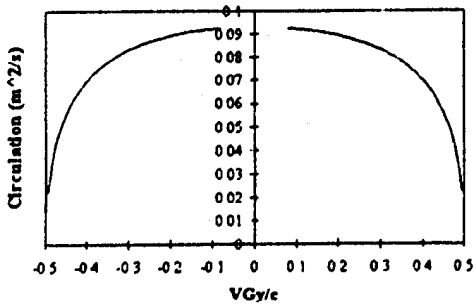

Fig. 3b. Circulation distribution over the wing

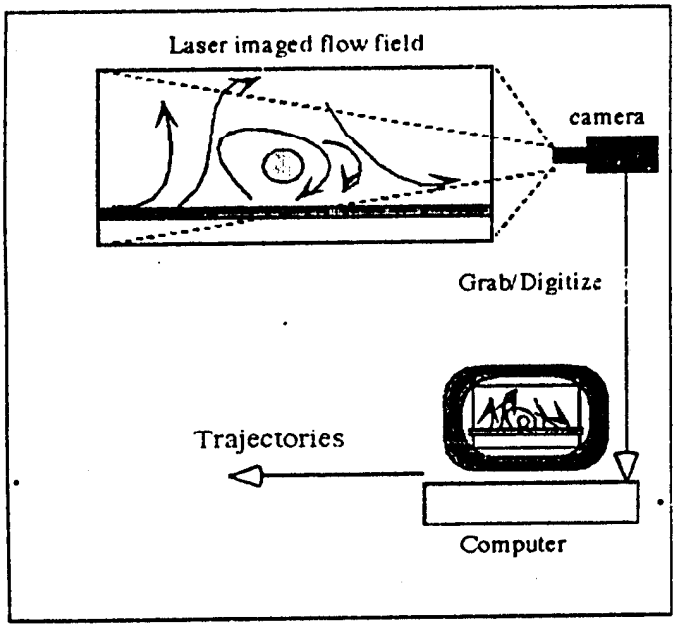

Fig. 2(b). Flow-visualization and data acquisition

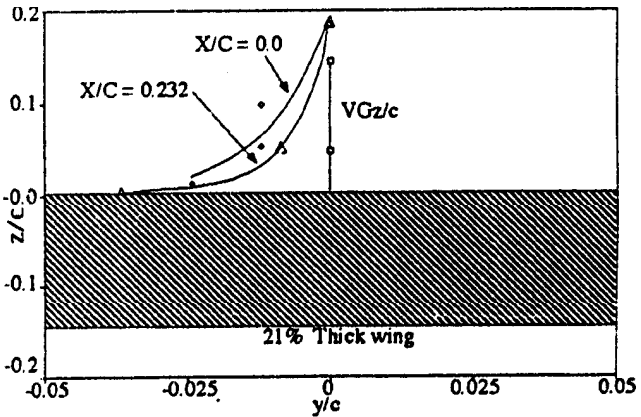

Fig.4. Vortex trajectories near the leading edge of the thick airfoil